

# QCD factorizations in $\gamma^*\gamma^* \rightarrow \rho_L^0\rho_L^0$

B. Pire<sup>a</sup>, M. Segond<sup>b</sup>, L. Szymanowski<sup>b,c,d</sup> and S. Wallon<sup>b</sup>

<sup>a</sup> CPHT<sup>1</sup>, École Polytechnique, 91128 Palaiseau, France

<sup>b</sup> LPT<sup>2</sup>, Université Paris-Sud, 91405-Orsay, France

<sup>c</sup> Université de Liège, B4000 Liège, Belgium

<sup>d</sup> Sołtan Institute for Nuclear Studies, Hoża 69, 00-681 Warsaw, Poland

## Abstract

We calculate the lowest order QCD amplitude, i.e. the quark exchange contribution, to the forward production amplitude of a pair of longitudinally polarized  $\rho$  mesons in the scattering of two virtual photons  $\gamma^*(Q_1)\gamma^*(Q_2) \rightarrow \rho_L^0\rho_L^0$ . We show that the scattering amplitude simultaneously factorizes in two quite different ways: the part with transverse photons is described by the QCD factorization formula involving the generalized distribution amplitude of two final  $\rho$  mesons, whereas the part with longitudinally polarized photons takes the QCD factorized form with the  $\gamma_L^* \rightarrow \rho_L^0$  transition distribution amplitude. Perturbative expressions for these, in general, non-perturbative functions are obtained in terms of the  $\rho$ -meson distribution amplitude.

---

<sup>1</sup>Unité mixte 7644 du CNRS

<sup>2</sup>Unité mixte 8627 du CNRS

# 1 Introduction

The exclusive reaction

$$\gamma^*(q_1)\gamma^*(q_2) \rightarrow \rho_L^0(k_1)\rho_L^0(k_2). \quad (1)$$

is a beautiful theoretical laboratory for the understanding of factorization properties of high energy QCD. In previous studies we emphasized the gluon exchange contribution which dominates in the very high energy (small- $x$ ) regime, both at the Born order [1] and in the resummed BFKL approach [2]. At lower scattering energy one can expect a non negligible contribution of quark exchange, since in the strong coupling  $g$  expansion, quark exchange processes appear at lower order, namely at order  $g^2$ , than the gluon exchange ones. The study of these quark exchanges processes is the main motivation of the present work. The Born order contribution with quark exchanges is described by the same set of diagrams which contribute to the scattering of real photons producing pions, e.g.  $\gamma\gamma \rightarrow \pi^+\pi^-$ , at large momentum transfer, studied long ago by Brodsky and Lepage [3] in the framework of the factorized form of exclusive processes at fixed angle [4], in which mesons are described by their light-cone distribution amplitudes (DAs). This is illustrated in Fig.1. In this sense our

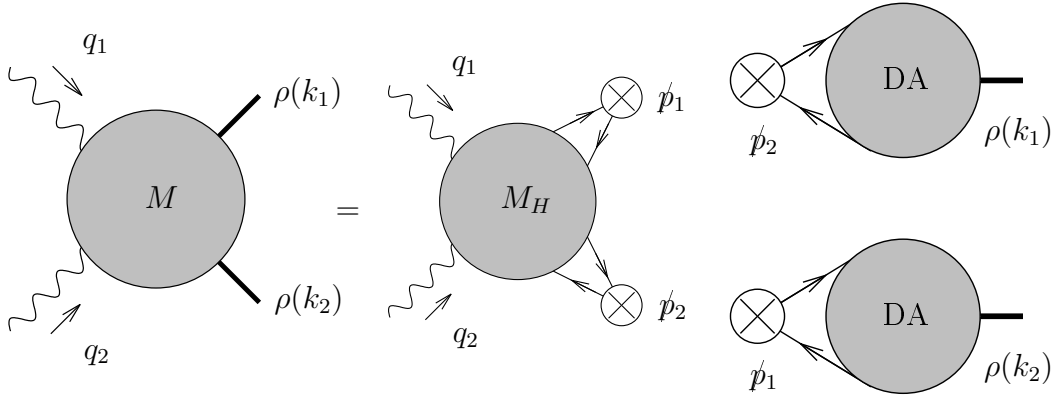


Figure 1: The amplitude of the process  $\gamma^*(Q_1)\gamma^*(Q_2) \rightarrow \rho_L^0(k_1)\rho_L^0(k_2)$  in the collinear factorization.

present study can be seen as a complement of Ref. [3] for the case of the scattering with virtual photons, i.e. with both, transverse and longitudinal polarizations, and in the forward kinematics (see also Ref. [5]). The virtualities  $Q_i^2 = -q_i^2$ ,  $i = 1, 2$ , supply the hard scale to the process (1) which justifies the use of the QCD collinear factorization methods and the description of  $\rho$  mesons by means of their distribution amplitudes.

We calculate in Sec. 3 within this scheme the scattering amplitude of (1) at Born level. At this stage we do not impose any additional conditions on the magnitudes of photon virtualities  $Q_i$ . Next, we turn to the study of two particular kinematical regions: (1) the region where the squared invariant mass of the two rho's  $W^2$  is much smaller than the largest photon virtualities, namely  $Q_1^2 \gg W^2$  (or  $Q_2^2 \gg W^2$ ), with  $Q_1$  and  $Q_2$  being not parametrically close, see Sec. 4 for more details, and (2) the region where photon virtualities are strongly ordered, that is  $Q_1^2 \gg Q_2^2$  (or  $Q_2^2 \gg Q_1^2$ ). We will show in Sec. 4 that in the region (1) the amplitude with transverse photons factorizes in a hard subprocess and a Generalized Distribution Amplitude [6, 7], up to corrections of order  $W^2/Q_1^2$  (resp.  $W^2/Q_2^2$ ). In the region (2) the amplitude with longitudinal photons factorizes in a hard

subprocess and a Transition Distribution Amplitude [8], up to corrections of order  $Q_2^2/Q_1^2$  (resp.  $Q_1^2/Q_2^2$ ), as is shown in Sec. 5. These two domains have a non empty intersection as

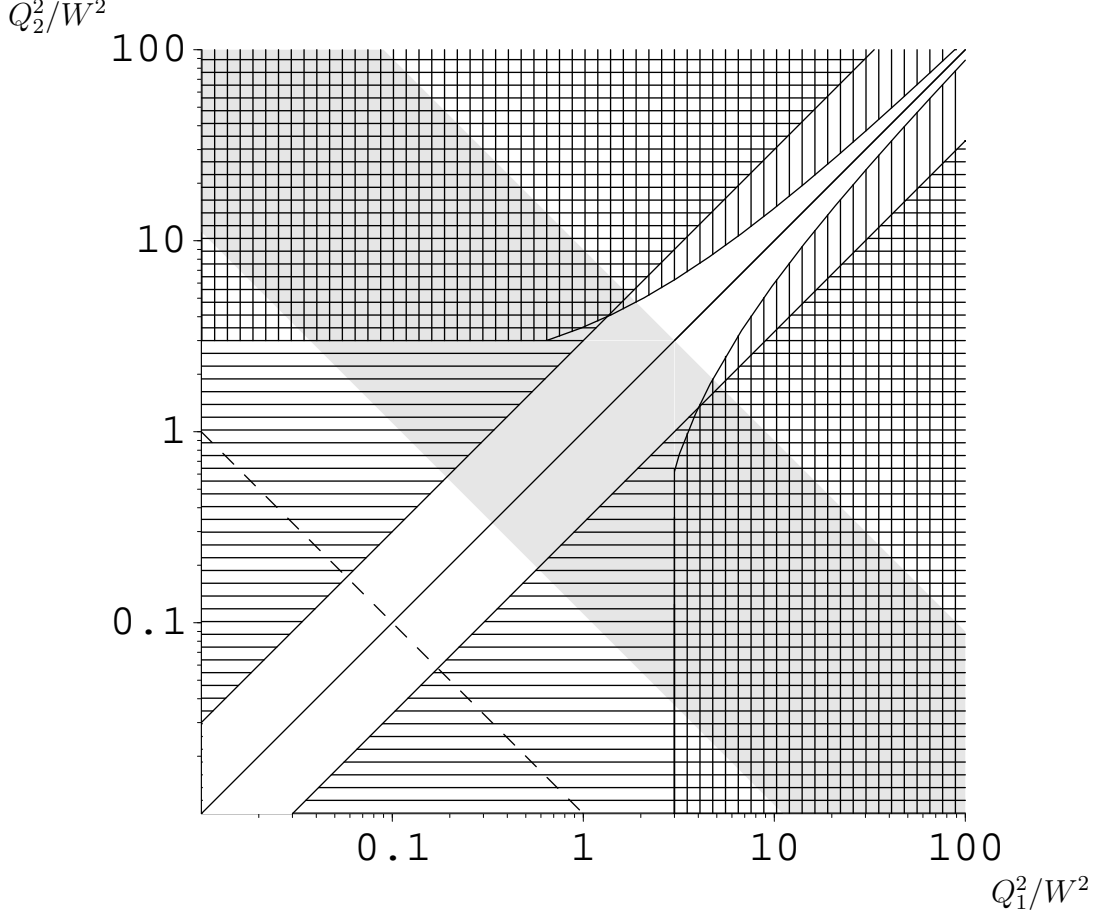


Figure 2: Different kinematical regions. In the domain (1), denoted with vertical lines, the QCD factorization with a GDA is justified. This region is the union of two disconnected domains: the lower right one is given by the conditions  $1 - Q_2^2/s \geq c(1 - Q_1^2/s)$  and  $Q_1^2/W^2 \geq c$  while the upper left one is given by  $1 - Q_1^2/s \geq c(1 - Q_2^2/s)$  and  $Q_2^2/W^2 \geq c$ ,  $c$  being arbitrary large. In the domain (2), denoted with horizontal lines, the QCD factorization with a TDA is justified. It corresponds to  $Q_1^2/Q_2^2 \geq c$  or  $Q_1^2/Q_2^2 \leq 1/c$ . In the intersecting domain, both factorizations are valid, while in the region without any lines, no factorization neither in terms of GDA nor TDA is established. For illustration, we choose  $c = 3$ . The grey band represents the domain where the Born order amplitudes with transverse and longitudinal photon, calculated directly as in Sec. 3, have comparable magnitudes. In the upper (lower) corner the transverse (resp. longitudinal) polarizations give dominant contribution. Below the dashed line is the perturbative Regge domain.

shown in Fig.2. In this intersection, we get two factorisation formulas for both polarizations of the photons,  $\gamma_T^* \gamma_T^* \rightarrow \rho_L \rho_L$  and  $\gamma_L^* \gamma_L^* \rightarrow \rho_L \rho_L$ . Fig. 2 illustrates also that the collinear QCD factorization with GDA or TDA is not demonstrated by our analysis in the limited region where the virtualities  $Q_i^2$  are parametrically close. In this figure, the different domains where the transverse or longitudinal amplitudes dominates are displayed. Finally, Fig. 2 shows the perturbative Regge domain, corresponding to the large  $W^2$  limit.

In this paper we concentrate ourselves, for simplicity, on the case of longitudinally polarized rho mesons. In this spirit, the longitudinal rho pairs and the pion pairs lead to similar

results. Our study is closely related to the perturbative limit of the two-pion light-cone distribution amplitude performed in Ref. [5] for  $\gamma_T^* \gamma_T$  collisions in the GDA limit.

Thus, the question we investigate here is how the known QCD factorization formulas emerge from a Born order calculation in both the longitudinally polarized and transversally polarized photon cases. As a by product, we get a perturbative expression for the non-perturbative hadronic objects - the  $\rho\rho$  GDA and the  $\gamma^* \rightarrow \rho$  TDA - in terms of the  $\rho$ -meson distribution amplitude.

## 2 Kinematics

Let us fix the kinematics, which is quite simple in the forward regime that we are investigating. The inclusion of transverse momentum would not change dramatically our result but would necessitate the introduction of more complicated tensorial structures. We use a Sudakov decomposition with two lightlike vectors  $p_1$  and  $p_2$  with  $2p_1 \cdot p_2 = s$  and write the photon momenta as

$$q_1 = p_1 - \frac{Q_1^2}{s} p_2 \quad q_2 = p_2 - \frac{Q_2^2}{s} p_1 , \quad (2)$$

and the final meson momenta as

$$k_1 = (1 - \frac{Q_2^2}{s}) p_1 \quad k_2 = (1 - \frac{Q_1^2}{s}) p_2 . \quad (3)$$

The positivity of energy of produced  $\rho$ 's requires that  $s \geq Q_i^2$ . The usual invariant  $W^2$  is defined as

$$W^2 = (q_1 + q_2)^2 = (k_1 + k_2)^2 = s(1 - \frac{Q_1^2}{s})(1 - \frac{Q_2^2}{s}) , \quad (4)$$

or

$$s = \frac{1}{2} [Q_1^2 + Q_2^2 + W^2 + \lambda(Q_1^2, Q_2^2, -W^2)] , \quad (5)$$

with  $\lambda(x, y, z) \equiv \sqrt{x^2 + y^2 + z^2 - 2xy - 2xz - 2zy}$ , while the minimum squared momentum transfer is

$$t_{min} = (q_2 - k_2)^2 = (q_1 + k_1)^2 = -\frac{Q_1^2 Q_2^2}{s} . \quad (6)$$

Note that, contrarily to the case studied in Ref. [3, 5],  $t_{min}$  may not be large with respect to  $\Lambda_{QCD}^2$ , depending on the respective values of  $Q_1^2$ ,  $Q_2^2$  and  $W^2$ .

## 3 The Born order amplitude

The scattering amplitude  $\mathcal{A}$  of the process (1) can be written in the form

$$\mathcal{A} = T^{\mu\nu} \epsilon_\mu(q_1) \epsilon_\nu(q_2) , \quad (7)$$

where the tensor  $T^{\mu\nu}$  has in the above kinematics a simple decomposition which is consistent with Lorentz covariance and electromagnetic gauge invariance

$$T^{\mu\nu} = \frac{1}{2} g_T^{\mu\nu} (T^{\alpha\beta} g_{T\alpha\beta}) + (p_1^\mu + \frac{Q_1^2}{s} p_2^\mu) (p_2^\nu + \frac{Q_2^2}{s} p_1^\nu) \frac{4}{s^2} (T^{\alpha\beta} p_{2\alpha} p_{1\beta}) , \quad (8)$$

and where  $g_T^{\mu\nu} = g^{\mu\nu} - (p_1^\mu p_2^\nu + p_1^\nu p_2^\mu)/(p_1 \cdot p_2)$ . The first term on the rhs of Eq. (8) contributes in the case of transversely polarized photons, the second one for longitudinally polarized virtual photons. The longitudinally polarized  $\rho^0$ -meson DA  $\phi(z)$  is defined by the non-local correlator (for simplicity of notation we omit the Wilson line)

$$\langle \rho_L^0(k) | \bar{q}(x) \gamma^\mu q(0) | 0 \rangle = \frac{f_\rho}{\sqrt{2}} k^\mu \int_0^1 dz e^{iz(kx)} \phi(z), \quad \text{for } q = u, d, \quad (9)$$

proportional to the coupling constant  $f_\rho$ .

The Born order contribution to the amplitude (7) is calculated in a similar way as in the classical work of Brodsky-Lepage [3] but in very different kinematics. In our case the virtualities of photons supply the hard scale, and not the transverse momentum transfer. Moreover, we consider the forward kinematics for simplicity. Relying on the collinear approximation, the momenta of the quarks and antiquarks which constitute the rho mesons can be written as

$$\begin{aligned} \ell_1 &\sim z_1 k_1, & \ell_2 &\sim z_2 k_2 \\ \tilde{\ell}_1 &\sim \bar{z}_1 k_1, & \tilde{\ell}_2 &\sim \bar{z}_2 k_2. \end{aligned} \quad (10)$$

The number of possible diagrams is 20. They can be organized into two classes. The first class corresponds to the diagrams where the two virtual photons couple to two different quark lines. In this way, one can build 8 different diagrams, as illustrated in Fig.3. The second

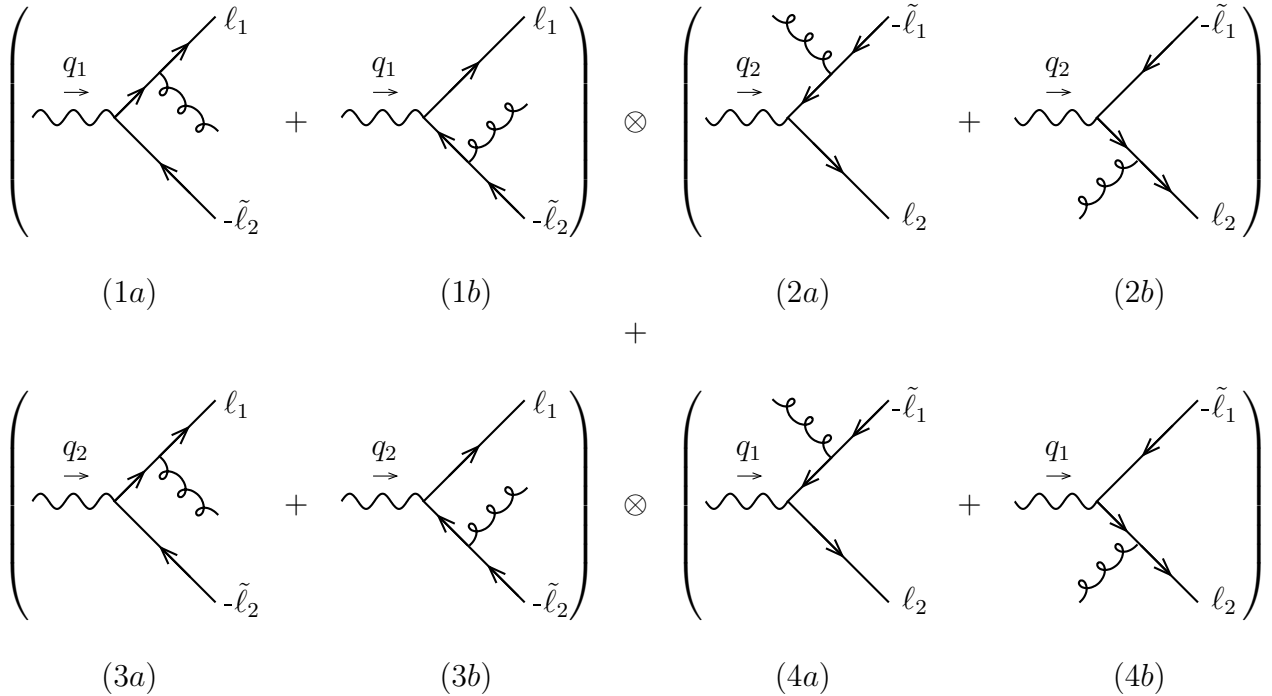


Figure 3: Feynman diagrams contributing to  $M_H$ , in which the virtual photons couple to different quark lines.

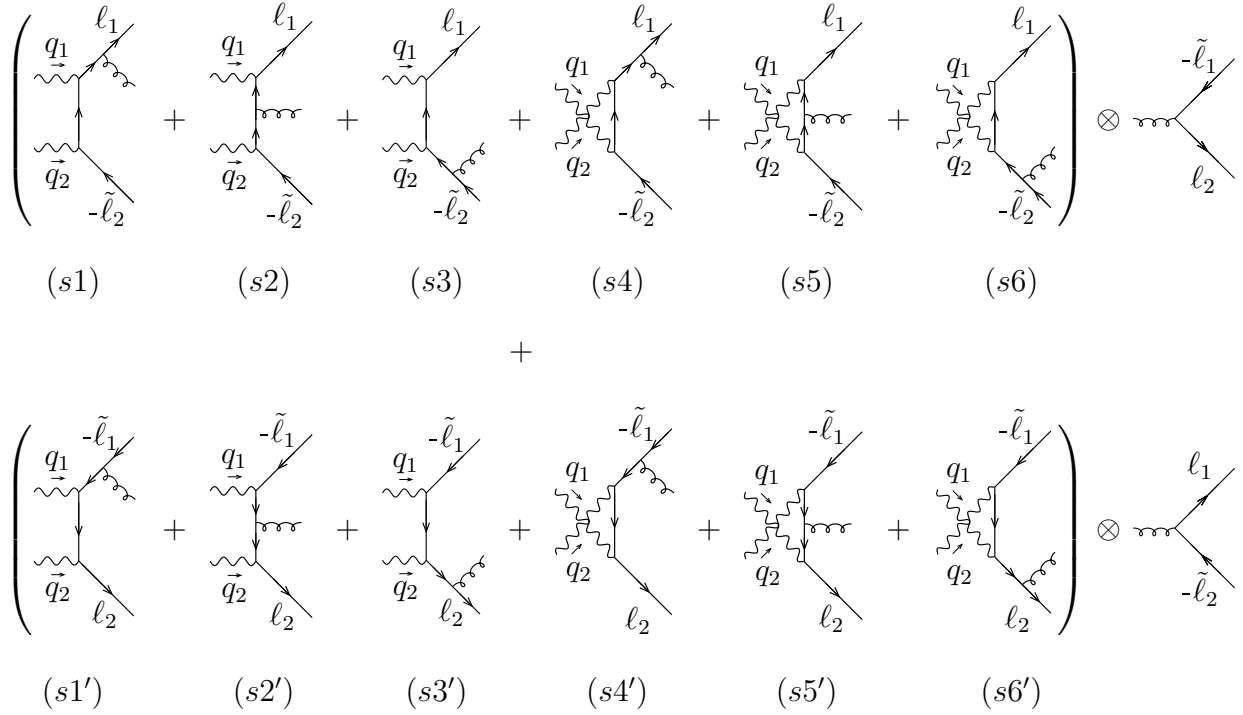


Figure 4: Feynman diagrams contributing to  $M_H$ , in which the virtual photons couple to a single quark line.

class of diagrams corresponds to the one where the two virtual photons are coupled to the same quark line, resulting into 12 different contributions, as illustrated in Fig.4.

Let us first focus on the case of longitudinally polarized photon. Their polarization read

$$\epsilon_{\parallel}(q_1) = \frac{1}{Q_1}q_1 + \frac{2Q_1}{s}p_2 \quad \text{and} \quad \epsilon_{\parallel}(q_2) = \frac{1}{Q_2}q_2 + \frac{2Q_2}{s}p_1. \quad (11)$$

Due to the gauge invariance of the total amplitude, when computing each Feynman diagrams, one can make use of the fact that the longitudinal polarization of photon 1 (resp. 2) can be effectively considered as proportional to  $p_2$  (resp.  $p_1$ ), in accordance with the structure of the second term of Eq.(8). One then readily sees that in the kinematics we are investigating, the only diagrams which are non zero in the Feynman gauge are the diagrams  $(1b) \otimes (2a)$ ,  $(3a) \otimes (4b)$  on the one hand, and  $(s2)$ ,  $(s2')$  on the other hand. Thus, only the four diagrams illustrated in Fig.5 contribute.

In the case of transversally polarized virtual photons, described by the first term in Eq.(8), one needs to contract the two polarization indices through the two dimensional identity tensor  $g_{\mu\nu}^T$ . The four non vanishing graphs corresponding to the coupling of the photons to different quark lines are  $(1a) \otimes (2b)$ ,  $(1b) \otimes (2a)$ ,  $(3a) \otimes (4b)$  and  $(3b) \otimes (4a)$ . When considering the graphs corresponding to the coupling of the photons to the same quark line, the above mentioned contraction kills the graphs  $(s2)$ ,  $(s2')$  and  $(s5)$ ,  $(s5')$ , that is the graphs where the gluon is emitted from the quark connecting the two virtual photons. In this second class of diagrams, 8 diagrams thus remain. The whole set of twelve diagrams to be computed is shown in Fig.6.

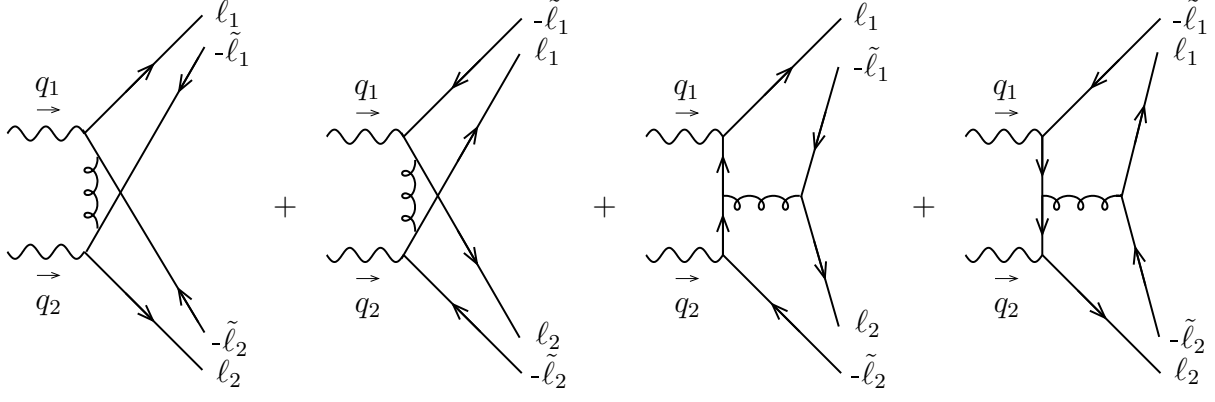


Figure 5: Feynman diagrams contributing to  $M_H$  in the case of longitudinally polarized virtual photons.

It should be noted that in the peculiar kinematics which is chosen here, the only diagrams which contribute both to the longitudinal and to the transverse virtual photon cases are  $(1b) \otimes (2a)$ ,  $(3a) \otimes (4b)$ , that is the two first diagrams of Fig.5 and Fig.6.

The scalar components of the scattering amplitude (8) read :

$$T^{\alpha\beta} g_{T\alpha\beta} = -\frac{e^2(Q_u^2 + Q_d^2) g^2 C_F f_\rho^2}{4 N_c s} \int_0^1 dz_1 dz_2 \phi(z_1) \phi(z_2) \quad (12)$$

$$\begin{aligned} & \times \left\{ 2 \left(1 - \frac{Q_2^2}{s}\right) \left(1 - \frac{Q_1^2}{s}\right) \left[ \frac{1}{(z_2 + \bar{z}_2 \frac{Q_1^2}{s})^2 (z_1 + \bar{z}_1 \frac{Q_2^2}{s})^2} + \frac{1}{(\bar{z}_2 + z_2 \frac{Q_1^2}{s})^2 (\bar{z}_1 + z_1 \frac{Q_2^2}{s})^2} \right] + \right. \\ & \left. \left( \frac{1}{\bar{z}_2 z_1} - \frac{1}{\bar{z}_1 z_2} \right) \left[ \frac{1}{1 - \frac{Q_2^2}{s}} \left( \frac{1}{\bar{z}_2 + z_2 \frac{Q_1^2}{s}} - \frac{1}{z_2 + \bar{z}_2 \frac{Q_1^2}{s}} \right) - \frac{1}{1 - \frac{Q_1^2}{s}} \left( \frac{1}{\bar{z}_1 + z_1 \frac{Q_2^2}{s}} - \frac{1}{z_1 + \bar{z}_1 \frac{Q_2^2}{s}} \right) \right] \right\} \\ T^{\alpha\beta} p_{2\alpha} p_{1\beta} &= -\frac{s^2 f_\rho^2 C_F e^2 g^2 (Q_u^2 + Q_d^2)}{8 N_c Q_1^2 Q_2^2} \int_0^1 dz_1 dz_2 \phi(z_1) \phi(z_2) \quad (13) \\ & \times \left\{ \frac{(1 - \frac{Q_1^2}{s})(1 - \frac{Q_2^2}{s})}{(z_1 + \bar{z}_1 \frac{Q_2^2}{s})(z_2 + \bar{z}_2 \frac{Q_1^2}{s})} + \frac{(1 - \frac{Q_1^2}{s})(1 - \frac{Q_2^2}{s})}{(\bar{z}_1 + z_1 \frac{Q_2^2}{s})(\bar{z}_2 + z_2 \frac{Q_1^2}{s})} + \frac{1}{z_2 \bar{z}_1} + \frac{1}{z_1 \bar{z}_2} \right\}, \end{aligned}$$

where  $Q_u = 2/3$  ( $Q_d = -1/3$ ) denote the charge of the quark  $u$  ( $d$ ),  $C_F = (N_c^2 - 1)/(2N_c)$  and  $N_c = 3$ .

The above results are obtained for arbitrary values of the photon virtualities  $Q_i$ . A closer look into formulas (7-13) leads to the conclusion that all integrals over quarks momentum fractions  $z_i$  are convergent due to the non-zero values of  $Q_i$ . Further inspection of the amplitudes (7-13) reveals that the transverse photon part has a behaviour like  $1/W^2$  while the longitudinal photon part behaves like  $1/(Q_1 Q_2)$ . This shows that their relative magnitude is different in each region (1) and (2) discussed in Sec. 1.

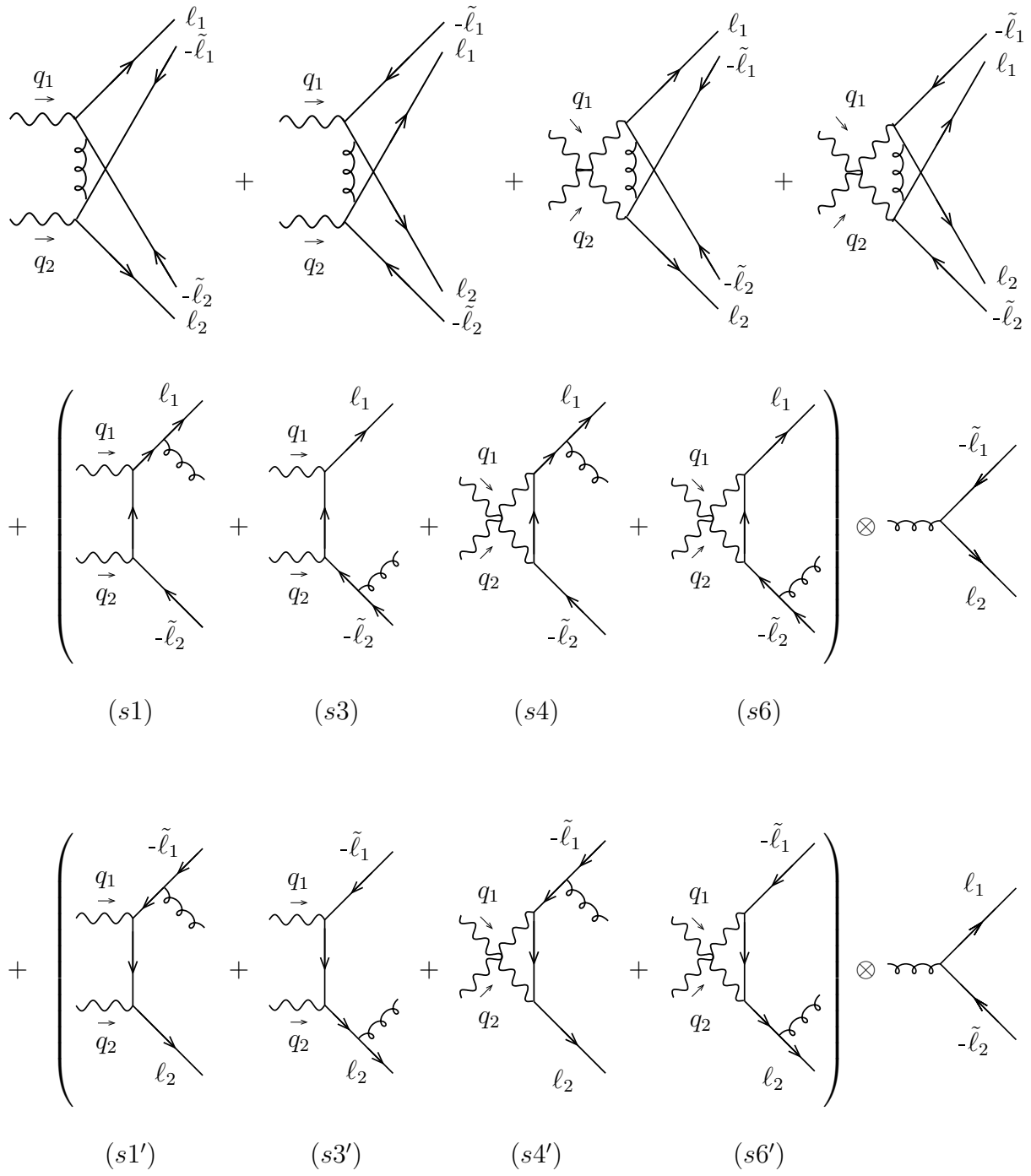


Figure 6: Feynman diagrams contributing to  $M_H$  in the case of transversally polarized virtual photons.



## 4 $\gamma_T^* \gamma_T^* \rightarrow \rho_L^0 \rho_L^0$ in the generalized Bjorken limit

Let us first focus on the region where the scattering energy  $W$  is small in comparison with the highest photon virtuality  $Q_1$

$$\frac{W^2}{Q_1^2} = \frac{s}{Q_1^2} \left(1 - \frac{Q_1^2}{s}\right) \left(1 - \frac{Q_2^2}{s}\right) \approx 1 - \frac{Q_1^2}{s} \ll 1, \quad (14)$$

which leads to the kinematical conditions very close to the ones considered in Ref. [6, 7] for the description of  $\gamma^* \gamma \rightarrow \pi\pi$  near threshold. In Ref. [6, 7] it was shown that with initial transversally polarized photons, the scattering amplitude factorizes at leading twist as the convolution of a perturbatively calculable coefficient function and a generalized distribution amplitude (GDA). We will recover a similar type of factorization with a GDA of the expression (12) also in the case of our process (1), as illustrated in Fig.7, provided  $Q_1$  and  $Q_2$  are not

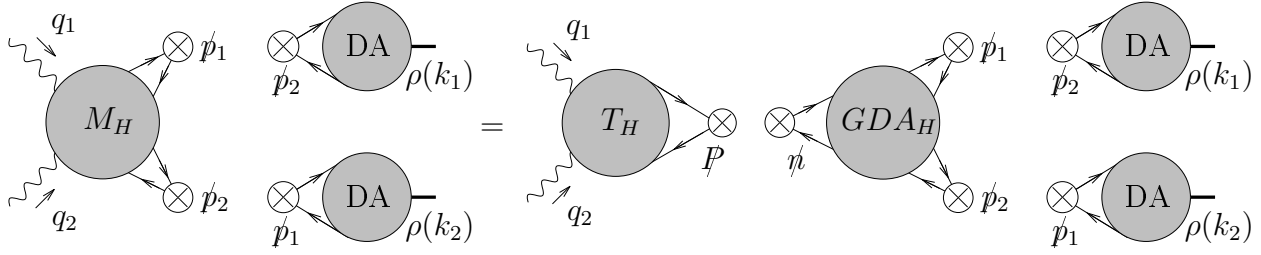


Figure 7: Factorisation of the amplitude in terms of a GDA.

parametrically close, i.e.

$$1 - \frac{Q_1^2}{s} \ll 1 - \frac{Q_2^2}{s}. \quad (15)$$

Indeed, in the scaling limit (14) with (15), the contribution of the four cats-ears diagrams (i.e. the first line of Fig.6), which corresponds to the second line of (12), is subdominant and the dominant contribution is given by the last term in (12), i.e.

$$T^{\alpha\beta} g_{T\alpha\beta} \approx \frac{e^2(Q_u^2 + Q_d^2) g^2 C_F f_\rho^2}{4 N_c W^2} \int_0^1 dz_1 dz_2 \phi(z_1) \phi(z_2) \quad (16)$$

$$\left( \frac{1}{\bar{z}_2 z_1} - \frac{1}{\bar{z}_1 z_2} \right) \left( \frac{1}{\bar{z}_1 + z_1 \frac{Q_2^2}{s}} - \frac{1}{z_1 + \bar{z}_1 \frac{Q_2^2}{s}} \right).$$

The virtuality  $Q_2$  plays in the expression (16) the role of a regulator of the end-point singularities (compare with [7]). Before recovering each factor of the factorized equation (16) by a direct calculation, let us discuss the physics which is behind. In Fig.6, the diagrams which contribute in the scaling region (14) with (15) are (s3), (s3') and (s6), (s6'). The sum of these four diagrams factorizes into a hard part convoluted with a soft (but still perturbative) part. Indeed, the typical virtuality of the hard quark connecting the two virtual photons is of the order of  $Q_1^2$  for graphs (s3), (s3') and  $s$  for graphs (s6), (s6'), while the virtuality of the quark connecting the emitted gluon to the virtual photon is of the order of  $W^2$ , which is negligible in the scaling region with respect to  $Q_1^2$  and  $s$ .

Let us now recall the definition of the leading twist GDA for  $\rho_L^0$  pair. We introduce the vector  $P = k_1 + k_2 \approx p_1$ , whereas the field coordinates are the ray-vectors along the light-cone direction  $n^\mu = p_2^\mu / (p_1 \cdot p_2)$ . In our kinematics the usual variable  $\zeta = (k_1 n) / (P n)$  characterizing the GDA equals  $\zeta \approx 1$ . Thus we define the GDA of the  $\rho_L^0$  pair  $\Phi_q(z, \zeta, W^2)$  by the formula

$$\begin{aligned} & \langle \rho_L^0(k_1) \rho_L^0(k_2) | \bar{q}(-\alpha n/2) \not{n} \left[ \int_{-\frac{\alpha}{2}}^{\frac{\alpha}{2}} dy n_\nu A^\nu(y) \right] q(\alpha n/2) | 0 \rangle \\ &= \int_0^1 dz e^{-i(2z-1)\alpha(nP)/2} \Phi^{\rho_L \rho_L}(z, \zeta, W^2), \quad q = u, d. \end{aligned} \quad (17)$$

Now we calculate the GDA  $\Phi_q(z, \zeta, W^2)$  in the Born order of the perturbation theory. First we show that the gluonic Wilson line does not give a contribution in our kinematics. For that expand the Wilson line and the S-matrix operator with quark-gluon interaction in (17) at the first order in  $g$ . We obtain (up to an irrelevant multiplicative factor)

$$n_\mu g^2 \int d^4v \langle \rho_L^0(k_1) \rho_L^0(k_2) | T[\bar{q}(-\alpha n/2) \gamma^\mu \left[ \int_{-\frac{\alpha}{2}}^{\frac{\alpha}{2}} dy n_\nu A^\nu(y) \right] q(\alpha n/2) \bar{q}(v) \not{A}(v) q(v)] | 0 \rangle \quad (18)$$

After applying the Fierz identity and ordering quark operators into two non-local correlators defining DA of  $\rho$ -mesons we obtain

$$n_\mu \langle \rho_L^0(k_1) | \bar{q}(-\alpha n/2) \gamma^\delta q(v) | 0 \rangle \langle \rho_L^0(k_2) | \bar{q}(v) \gamma^\sigma q(\alpha n/2) | 0 \rangle Tr[\gamma^\delta \gamma^\mu \gamma^\sigma \gamma^\beta] n_\beta + (k_1 \leftrightarrow k_2), \quad (19)$$

where we omitted the gluon propagator coming from the contraction of the two gauge fields. The original Wilson line results at this order in the presence of the vector  $n_\beta$  in the above expression. The only nonvanishing contribution at leading twist takes the form

$$\langle \rho_L^0(k_1) | \bar{q}(-\alpha n/2) \not{n} q(v) | 0 \rangle \langle \rho_L^0(k_2) | \bar{q}(v) \not{n} q(\alpha n/2) | 0 \rangle Tr[\not{p}_1 \not{n} \not{p}_1 \not{n}] + (k_1 \leftrightarrow k_2). \quad (20)$$

This is illustrated in Fig.8.

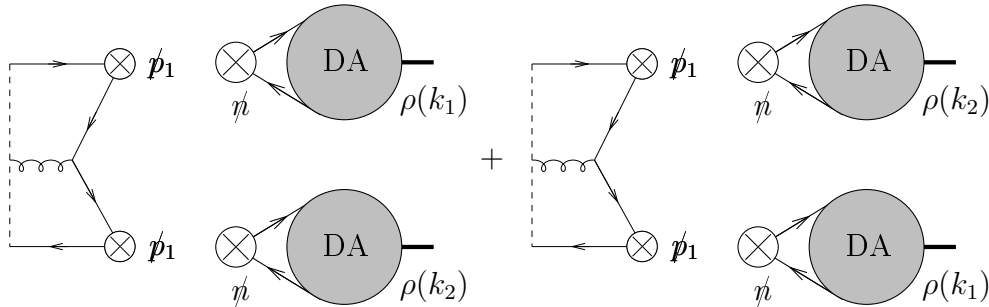


Figure 8: Wilson line contribution to the GDA, expressed as a convolution of a hard part with the DAs.

It equals zero since in our kinematics one of the matrix elements defining DA of  $\rho$ -meson vanishes.

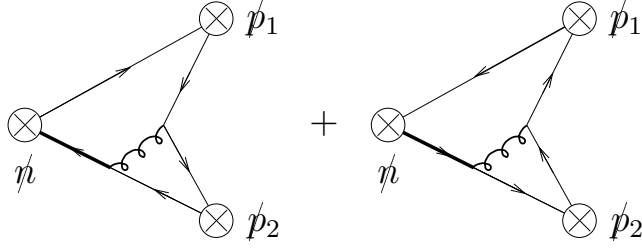


Figure 9: Non vanishing contributions to the hard part of the GDA at Born order. The quark and gluon bold lines correspond to propagators .

The remaining contributions to the correlator in (17) at order  $g^2$  are illustrated in Fig.9. It leads to the result

$$\Phi^{\rho_L \rho_L}(z, \zeta \approx 1, W^2) = -\frac{f_\rho^2 g^2 C_F}{2 N_c W^2} \int_0^1 dz_2 \phi(z) \phi(z_2) \left[ \frac{1}{z \bar{z}_2} - \frac{1}{\bar{z} z_2} \right]. \quad (21)$$

The hard part  $T_H$  of the amplitude corresponds to the diagrams shown in Fig.10. In the case

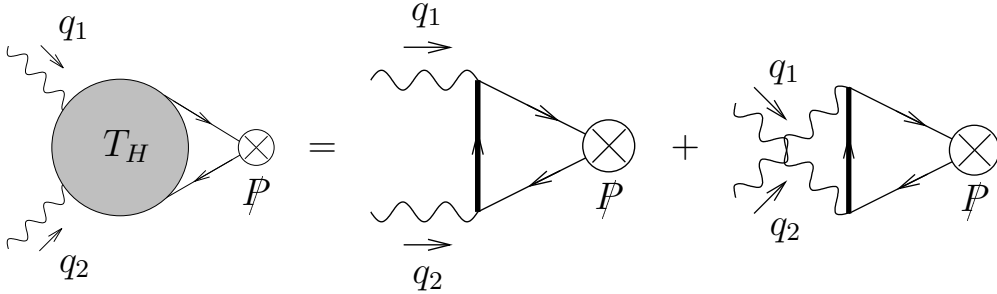


Figure 10: Expansion of the hard part  $T_H$  at  $g^2$  order. The bold lines correspond to quark propagators.

of a quark of a given flavour it equals

$$T_H(z) = -4 e^2 N_c Q_q^2 \left( \frac{1}{\bar{z} + z \frac{Q_2^2}{s}} - \frac{1}{z + \bar{z} \frac{Q_2^2}{s}} \right) \quad (22)$$

The Eqs. (21, 22) taken together with the flavour structure of  $\rho^0$  permit to write (16) in the form

$$T^{\alpha\beta} g_{T\alpha\beta} = \frac{e^2}{2} (Q_u^2 + Q_d^2) \int_0^1 dz \left( \frac{1}{\bar{z} + z \frac{Q_2^2}{s}} - \frac{1}{z + \bar{z} \frac{Q_2^2}{s}} \right) \Phi^{\rho_L \rho_L}(z, \zeta \approx 1, W^2), \quad (23)$$

which shows the factorization of  $T^{\alpha\beta} g_{T\alpha\beta}$  into the hard part and the GDA. The Eq. (23) is the limiting case for  $\zeta \rightarrow 1$  of the original equation derived by D. Müller et al [6].

## 5 $\gamma_L^* \gamma_L^* \rightarrow \rho_L^0 \rho_L^0$ in the generalized Bjorken limit

To analyse the case of longitudinally polarized photon scattering, let us now turn to another interesting limiting case where

$$Q_1^2 \gg Q_2^2. \quad (24)$$

In this regime, it has been advocated [8] that the amplitude with initial longitudinally polarized photons, should factorize as the convolution of a perturbatively calculable coefficient function and a  $\gamma \rightarrow \rho$  transition distribution amplitude (TDA) defined from the non-local quark correlator

$$\int \frac{dz^-}{2\pi} e^{-ixP^+z^-} \langle \rho(p_2) | \bar{q}(-z^-/2) \gamma^+ q(z^-/2) | \gamma(q_2) \rangle , \quad (25)$$

which shares many properties (including the QCD evolution equations) with the generalized parton distributions [6, 9] successfully introduced to describe deeply virtual Compton scattering.

The factorization properties of the scattering amplitude in this domain are conventionally described by using the now standard notations of GPDs. For that we rewrite the momenta of the particles involved in the process as

$$\begin{aligned} q_1 &= \frac{1}{1+\xi} n_1 - 2\xi n_2 , & k_1 &= \frac{1 - \frac{Q_2^2}{s}}{1+\xi} n_1 \\ q_2 &= -\frac{Q_2^2}{(1+\xi)s} n_1 + (1+\xi) n_2 , & k_2 &= (1-\xi) n_2 , \end{aligned} \quad (26)$$

where  $\xi$  is the skewedness parameter which equals  $\xi = Q_1^2/(2s - Q_1^2)$  (see also the formula (5) which relates  $s$  with the total scattering energy  $W$ ) and the new  $n_i$  Sudakov light-cone vectors are related to the  $p_i$ 's as

$$p_1 = \frac{1}{1+\xi} n_1 , \quad p_2 = (1+\xi) n_2 , \quad (27)$$

with  $p_1 \cdot p_2 = n_1 \cdot n_2 = s/2$ . We also introduce the average “target” momentum  $P$  and the momentum transfer  $\Delta$

$$P = \frac{1}{2}(q_2 + k_2) , \quad \Delta = k_2 - q_2 . \quad (28)$$

We still restrict our study to the strictly forward case with  $t = t_{min} = -2\xi Q_2^2/(1+\xi)$ .

In the region defined by Eq. (24) we can put  $Q_2 = 0$  inside  $\{\dots\}$  in the expression in Eq. (13), which results, in this approximation, in the formula:

$$\begin{aligned} &\int_0^1 dz_1 dz_2 \phi(z_1) \phi(z_2) \{\dots\} \\ &= \int_0^1 dz_1 dz_2 \phi(z_1) \phi(z_2) \left\{ \frac{(1-\xi)}{\bar{z}_1[\bar{z}_2(1+\xi) + 2\xi z_2]} + \frac{(1-\xi)}{z_1[z_2(1+\xi) + 2\xi \bar{z}_2]} + \frac{1}{z_2 \bar{z}_1} + \frac{1}{z_1 \bar{z}_2} \right\} . \end{aligned} \quad (29)$$

The terms in the  $\{\dots\}$  are ordered in accordance with diagrams shown in Fig.5.

Now our aim is to rewrite Eq. (29) in a form corresponding to the QCD factorization with a TDA, as illustrated in Fig.11.

For that we look more closely into diagrams contributing to each of the four terms in (29) from the point of view of such a factorization. For example, the second term in (29), corresponding to the second diagram shown in Fig.5, suggests the introduction of the new

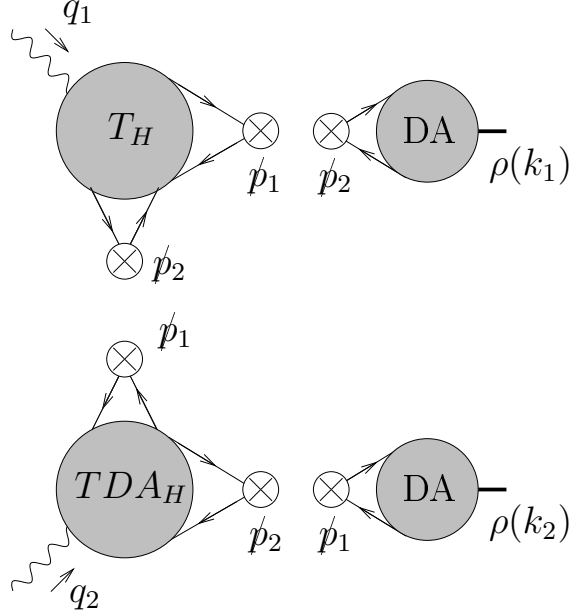


Figure 11: Factorization of the amplitude in terms of a TDA.

variable  $x$ , defined through  $z_2 = (x - \xi)/(1 - \xi)$ , with  $x \in [\xi, 1]$ , which results in the equality

$$\int_0^1 dz_2 \frac{\phi(z_2)(1 - \xi)}{z_1[z_2(1 + \xi) + 2\xi \bar{z}_2]} = \int_\xi^1 dx \frac{\phi\left(\frac{x - \xi}{1 - \xi}\right)}{z_1(x + \xi)}, \quad (30)$$

i.e. which corresponds to a part of the contribution from the DGLAP integration region of the amplitude with a factorized TDA. A similar analysis of all remaining terms permits to represent Eq. (29) in the form

$$\begin{aligned} & \int_0^1 dz_1 dz_2 \phi(z_1) \phi(z_2) \{ \dots \} \\ &= \int_{-1}^1 dx \int_0^1 dz_1 \phi(z_1) \left( \frac{1}{\bar{z}_1(x - \xi)} + \frac{1}{z_1(x + \xi)} \right) \\ & \times \left[ \Theta(1 \geq x \geq \xi) \phi\left(\frac{x - \xi}{1 - \xi}\right) - \Theta(-\xi \geq x \geq -1) \phi\left(\frac{1 + x}{1 - \xi}\right) \right], \end{aligned} \quad (31)$$

with the step function  $\Theta(a \geq x \geq b) = \Theta(a - x)\Theta(x - b)$ . This factorized expression suggests the identification of

$$\int_0^1 dz_1 \phi(z_1) \left( \frac{1}{\bar{z}_1(x - \xi)} + \frac{1}{z_1(x + \xi)} \right) \quad (32)$$

as the coefficient function  $T_H$  (up to a multiplicative factor), and of

$$T(x, \xi, t_{min}) \equiv N_c \left[ \Theta(1 \geq x \geq \xi) \phi\left(\frac{x - \xi}{1 - \xi}\right) - \Theta(-\xi \geq x \geq -1) \phi\left(\frac{1 + x}{1 - \xi}\right) \right] \quad (33)$$

as the  $\gamma_L^* \rightarrow \rho_L$  TDA.

To justify this interpretation we start from the hard part  $T_H(z_1, x)$  of the scattering amplitude, which appears in Fig.11, as illustrated at order  $g^2$  in Fig.12. It equals, for a

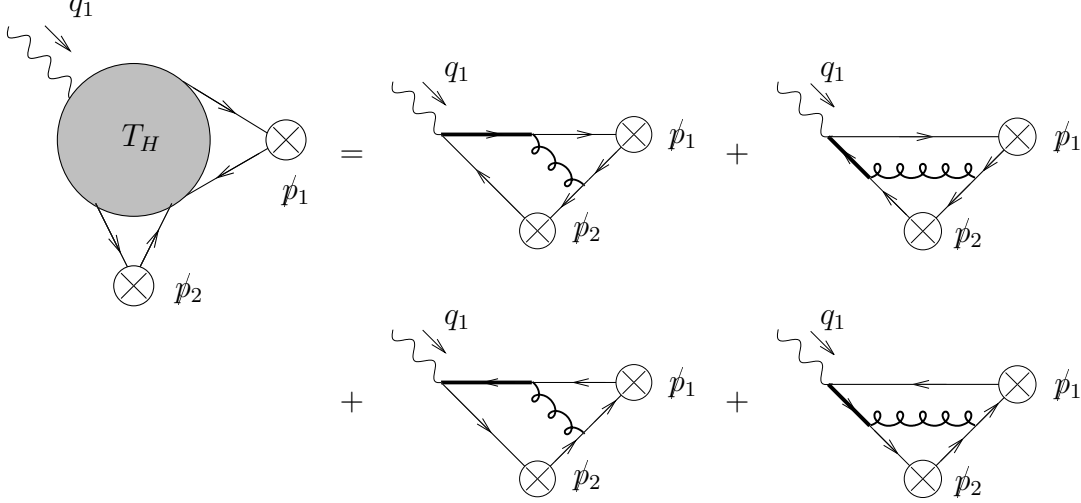


Figure 12: The hard part  $T_H$  at order  $g^2$ .

meson built from a quark with a single flavour,

$$T_H(z_1, x) = -i f_\rho g^2 e Q_q \frac{C_F \phi(z_1)}{2 N_c Q_1^2} \epsilon^\mu(q_1) \left( 2\xi n_{2\mu} + \frac{1}{1+\xi} n_{1\mu} \right) \times \left[ \frac{1}{z_1(x + \xi - i\epsilon)} + \frac{1}{\bar{z}_1(x - \xi + i\epsilon)} \right], \quad (34)$$

and obviously coincides with the hard part of the  $\rho$ -meson electroproduction amplitude. The tensorial structure  $2\xi n_2^\mu + \frac{1}{1+\xi} n_1^\mu = p_1^\mu + Q_1^2/s p_1^\mu$  coincides again with the one present in Eq.(8).

Passing to the TDA, let us consider the definition of  $\gamma_L^*(q_2) \rightarrow \rho_L^q(k_2)$  TDA,  $T(x, \xi, t_{min})$ , in which we assume that the meson is built from a quark with a single flavour,  $\rho_L^q(k_2) = \bar{q}q$ . The vector  $P = 1/2(q_2 + k_2) \approx n_2$  in our kinematics, and the ray-vector of coordinates is oriented along the light-cone vector  $n = n_1/(n_1 \cdot n_2)$ . The non-local correlator defining the TDA is given by the formula

$$\int \frac{dz^-}{2\pi} e^{ix(P \cdot z)} \langle \rho_L^q(k_2) | \bar{q}(-z/2) \hat{n} e^{-ieQ_q \int_{z/2}^{-z/2} dy_\mu A^\mu(y)} q(z/2) | \gamma^*(q_2) \rangle = \frac{e Q_q f_\rho}{P^+} \frac{2}{Q_2^2} \epsilon_\nu(q_2) \left( (1+\xi) n_2^\nu + \frac{Q_2^2}{s(1+\xi)} n_1^\nu \right) T(x, \xi, t_{min}), \quad (35)$$

in which we explicitly show the electromagnetic Wilson-line assuring the abelian gauge invariance of the non-local operator. On the contrary, for simplicity of notation, we omit the Wilson line required by the non-abelian QCD invariance since it does not play any role in this case. Note also that the factor  $(1+\xi) n_2^\nu + \frac{Q_2^2}{s(1+\xi)} n_1^\nu = p_2^\nu + \frac{Q_2^2}{s} p_1^\nu$  corresponds to a part of the tensorial structure of the second term in Eq. (8).

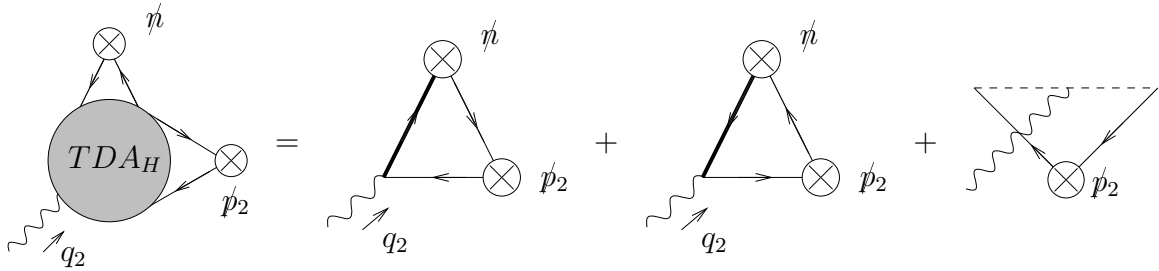


Figure 13: The hard part of the TDA at order  $e Q_q$ .

Now, the simple perturbative calculation of the matrix element in (35) in the lowest order in the electromagnetic coupling constant  $e$  leads to the expression for  $T(x, \xi, t_{min})$  given by Eq. (33). The contributing diagrams are drawn in Fig.13. In particular, the contribution to the rhs of (35) proportional to the vector  $n_1^\nu$  (or  $p_1^\nu$ ) corresponds to the contribution coming from the expansion of the electromagnetic Wilson line, illustrated by the last diagram in Fig.13.

Putting all factors together and restoring the flavour structure of the  $\rho^0$ , we obtain the factorized form involving a TDA, of the expression  $T^{\alpha\beta} p_{2\alpha} p_{1\beta}$  in Eq. (13) as

$$T^{\alpha\beta} p_{2\alpha} p_{1\beta} = -i f_\rho^2 e^2 (Q_u^2 + Q_d^2) g^2 \frac{C_F}{8N_c} \int_{-1}^1 dx \int_0^1 dz_1 \left[ \frac{1}{\bar{z}_1(x - \xi)} + \frac{1}{z_1(x + \xi)} \right] T(x, \xi, t_{min}) . \quad (36)$$

Note that in this perturbative analysis, only the DGLAP part of the TDA, with  $1 \geq |x| \geq \xi$ , contributes. This is a consequence of the support properties of the  $\rho$ -meson distribution amplitude.

## 6 Conclusions

Thus the perturbative analysis of the process  $\gamma^* \gamma^* \rightarrow \rho_L^0 \rho_L^0$  in the Born approximation leads to two different types of QCD factorization. We have shown that the polarization states of the photons dictate either the factorization involving a GDA or involving a TDA. Usually these two types of factorizations are applied to two different kinematical regimes. The arbitrariness in choosing values of photon virtualities  $Q_i^2$  shows that there may exist an intersection region where both types of factorization are simultaneously valid.

We have restricted our analysis to the case of longitudinally polarized  $\rho^0$ -mesons. In this way we have avoided the potential problems [10] due to the breaking of QCD factorization with GDA or TDA at the end-point region of the distribution amplitudes of transversally polarized vector mesons. It would be interesting to find out, whether a factorizing formula with GDA or TDA can also be obtained in this case.

Although we have restricted ourselves, for simplicity, to the forward kinematics, we believe that similar results may be obtained in a more general case. Also, we would like to mention that our results involving  $\rho^0$ -mesons can be generalized to the case of the production of a  $(\rho^+ \rho^-)$ -meson pair. On the theoretical side, in order to preserve the electromagnetic gauge invariance of the TDA  $\gamma^* \rightarrow \rho^\pm$ , one should modify the definition of the non-local correlator (35). This may be done by applying the Mandelstam approach [11], i.e. by

replacing the electromagnetically gauge invariant correlator (35) by the product of two effective electromagnetically gauge invariant quark fields  $q(z) \exp(i e_q \int_z^\infty dy n_\mu A^\mu(y))$ .

## Acknowledgments

This work is partially supported by the Polish Grant 1 P03B 028 28, the French-Polish scientific agreement Polonium, the triangular program ECO-NET, and the european Joint Research Activity I3 Program Hadronic Physics RII3-CT-506078. L.Sz. is a Visiting Fellow of the Fonds National pour la Recherche Scientifique (Belgium). We thank C. Ewerz, G. Korchemsky, J-P. Lansberg, D. Müller and A. Shuvaev for discussions.

## References

- [1] B. Pire, L. Szymanowski and S. Wallon, Eur. Phys. J. C **44** (2005) 545 [arXiv:hep-ph/0507038].
- [2] R. Enberg, B. Pire, L. Szymanowski and S. Wallon, Eur. Phys. J. C **45** (2006) 759 [arXiv:hep-ph/0508134].
- [3] S. J. Brodsky and G. P. Lepage, Phys. Rev. D **24** (1981) 1808.
- [4] G.P. Lepage and S.J. Brodsky, Phys. Lett. **B87**, 359 (1979); A.V. Efremov and A.V. Radyushkin, Phys. Lett. **B94**, 245 (1980).
- [5] M. Diehl, T. Feldmann, P. Kroll and C. Vogt, Phys. Rev. D **61** (2000) 074029 [arXiv:hep-ph/9912364].
- [6] D. Müller, D. Robaschik, B. Geyer, F. M. Dittes, J. Hořejši, Fortsch. Phys. **42**, 101 (1994);
- [7] M. Diehl, T. Gousset, B. Pire and O. Teryaev, Phys. Rev. Lett. **81**, 1782 (1998); M. Diehl, T. Gousset and B. Pire, Phys. Rev. D **62**, 073014 (2000); I. V. Anikin, B. Pire and O. V. Teryaev, Phys. Rev. D **69**, 014018 (2004).
- [8] B. Pire and L. Szymanowski, Phys. Rev. D **71** (2005) 111501; Phys. Lett. B **622** (2005) 83; J. P. Lansberg, B. Pire and L. Szymanowski, Phys. Rev. D **73** (2006) 074014 [arXiv:hep-ph/0602195].
- [9] X. Ji, Phys. Rev. Lett. **78**, 610 (1997); Phys. Rev. **D55**, 7114 (1997); A. V. Radyushkin, Phys. Rev. D **56**, 5524 (1997); J. Blümlein, B. Geyer and D. Robaschik, Phys. Lett. **B406**, 161 (1997); For a review, see M. Diehl, Phys. Rept. **388**, 41 (2003) and references therein.
- [10] L. Mankiewicz and G. Piller, Phys. Rev. D **61** (2000) 074013 [arXiv:hep-ph/9905287]; I. V. Anikin and O. V. Teryaev, Phys. Lett. B **554** (2003) 51 [arXiv:hep-ph/0211028].
- [11] S. Mandelstam, Annals Phys. **19**, 1 (1962).